Title: "A New Numerical Modeling Approach for Sound Propagation and Generation: the Lattice Boltzmann Method"

Authors:
M. Emin Kutay[1], Katherine Petros[2] and Salih Kocak[3]

[1] Assistant Professor
Michigan State University
Department of Civil and Environmental Engineering
East Lansing, Michigan, 48824-1226
kutay@egr.msu.edu
Tel: 517-353-9297 , Fax: 517- 432-1827

[2] Team Leader
Pavement Design & Performance Modeling Team
Turner-Fairbank Highway Research Center
Federal Highway Administration
6300 Georgetown Pike, Rm. F209
McLean, VA 22101-2296
E-mail: Katherine.Petros@fhwa.dot.gov
Tel: 202-493-3154, Fax: 202-493-3161

[2] Research Assistant
Michigan State University
Department of Civil and Environmental Engineering
East Lansing, Michigan, 48824-1226
kocaksal@msu.edu
Tel: 517-352-8006, Fax: 517- 432-1827

Offered for Review by
ADC40 - Committee on Transportation Related Noise and Vibration
Transportation Research Board
89th Annual Meeting
January 10-14, 2010
Washington, D.C.

ABSTRACT
Noise pollution is a growing concern in the United States and other countries. While there are many sources of noise, traffic noise is a major portion of total noise in the environment. A major component of traffic noise is the sound generated by the interaction of tires with the roadway. At high speeds, (>30 miles/hr) tire/pavement noise overshadows the noise from other sources in the vehicle. This paper presents a novel sound propagation and generation modeling technique that can be used in roadway applications including environmental impact studies of roadways and other noise sources, development of noise maps, and barrier design …etc. The model also has capability of simulating generation of sound. The model is based on one of the most efficient computational fluid dynamic techniques, the Lattice Boltzmann (LB) method. Unlike existing wave propagation models, this model simulates air pressure fluctuations (i.e., sound waves) at the tire/pavement interface by solving the Navier-Stokes equations for air. The details of the LB method and its validation using analytical solutions and laboratory measurements have been given. Furthermore, several example applications of LB method for sound propagation as well as sound generation problems have been presented.

Keywords:
Tire/pavement noise, Lattice Boltzmann Method, Modeling sound propagation

INTRODUCTION

Noise pollution due to the transportation infrastructure significantly influences the quality of life throughout the world. While there are many sources of noise, traffic noise is a major portion of total noise in the environment. There are several sources of roadway noise including the engine (power train), exhaust, aerodynamic flow and tire-roadway interaction. After certain speeds, the noise originating from the tire-roadway interaction becomes more dominant than other vehicle noise sources. In the case of cars, this limit is approximately 40 km/h, for trucks, it is about 70 km/h. In recent years, with the advent of quieter engines, the noise limit values for the vehicles have been considerably reduced. Therefore, the tire-roadway noise source is now of greater significance.

In order to meet the public demand, noise walls are typically constructed on the sides of roadways to prevent the unwanted sound waves travel towards the residential areas. However, this is a very costly measure. Noise walls can cost up to $1.0-$1.5 million per mile (only one side of the road). Building quieter pavements is anticipated to be a more economic way of addressing the highway noise problem. Optimization of characteristics of pavements for reduced noise, without adversely affecting their long term performance and public safety is a key to the success of designing quiet pavements. One of the major factors influencing the tire/pavement noise generation is the texture of pavement surface *(1)*. Recent studies have primarily focused on measurement of texture using both 2D and 3D laser-based techniques *(2)*. Then, correlation between tire/pavement noise and certain parameters representing macro-texture (e.g., mean profile depth) have been developed *(2)*. While surface texture significantly influence the generation of sound due to tire/pavement interaction, it also has a significant influence on the propagation of the sound.

One of the quietest pavements reported in the literature is the porous pavements. Due to the interconnected void structure, the sound waves caused by the tire/pavement interaction can penetrate into the pavement. This minimizes the waves reflected from the surface, which propagate to the environment. However, one of the important challenges associated with the porous pavements is their durability. Fine particles on the roadways can quickly clog the voids, reducing pavement's capability to absorb noise. The design air void level and type and shape of the aggregates affecting the surface area and interconnectivity of the pores can be crucial in the acoustic durability of porous pavements. Using field or laboratory methods, it can be time consuming and costly to study the effects of numerous variables such as surface texture, pore structure parameters (of porous pavements), material properties of pavements on the generation and propagation of noise. With the aid of an efficient and accurate numerical model, these factors can be studied rapidly and with minimal cost.

This paper presents a novel technique to model the propagation of sound waves using one of the most efficient computational fluid dynamics techniques, the Lattice Boltzmann (LB) method. The LB method is an explicit solution of time dependent propagation of air molecules, allowing computation and visualization of movement of sound waves in real-time. Unlike existing wave propagation models, this model simulates air pressure fluctuations (i.e., sound waves) at the tire/pavement interface by solving the Navier-Stokes equations for air. Another advantage of the LB model implemented in this study is that the input to the model is directly the black and white (binary) images of the geometries. Following sections describes the details of the LB method and its validation using analytical solutions and laboratory measurements. Furthermore, several example applications of LB method for sound propagation as well as sound generation problems are presented.

NUMERICAL MODELING OF SOUND GENERATION AND PROPAGATION

Sound is generated by pressure fluctuations in air, and since air is simply a fluid, computational fluid dynamics (CFD) techniques can theoretically be utilized to model the propagation of sound waves. One of the most efficient CFD methods is the Lattice Boltzmann (LB) method, which is based on molecular dynamics and directly simulates the air particle movement and their interaction. In this study, the LB method was implemented to explore the possibility of its application to model tire/pavement noise propagation as well as generation.

Lattice Boltzmann Method

The LB method has emerged as a versatile alternative to traditional finite element and finite difference Navier-Stokes solvers *(3)*. The LB method approximates the continuous Boltzmann equation by discretizing physical space with lattice nodes and velocity space by a set of microscopic velocity vectors *(4),(5)*. The time- and space-averaged microscopic movements of fluid particles are modeled using molecular populations called distribution function. The distribution function defines the density and velocity of fluid molecules at each lattice node at each time step. Fluid particles travel on the lattice nodes based on the magnitude and direction of the distribution function components. Specific particle interaction rules are set so that the Navier-Stokes equations are satisfied. The governing equations and detailed explanation of the LB method can be found in *(3)*.

An illustration of generation of lattice nodes for a given geometry and set of microscopic velocity vectors for the D2Q9 model is shown in Figure 1. As shown in Figure 1, uniformly spaced lattice nodes represent the voids and the solids. In LB method, microscopic velocities are defined for propagation of fluid molecules (Figure 1d), however, these are only used during propagation to neighboring nodes. The *macroscopic* velocity of the fluid at the node is continuous (i.e., can be in any direction as shown in Figure 1d). The time- and space-averaged microscopic movements of particles are modeled using molecular populations called the distribution function, which defines the density and velocity at each lattice node. Specific particle interaction rules are set so that the Navier-Stokes equations are satisfied. The time dependent movement of fluid particles at each lattice node satisfies the following particle propagation equation:

$$\mathrm{F}_i(\mathbf{x}+\mathbf{e}_i, t+1) = \mathrm{F}_i(\mathbf{x}, t) - \frac{1}{\tau}\left[\mathrm{F}_i(\mathbf{x}, t) - \mathrm{F}_i^{eq}(\mathbf{x}, t)\right] \qquad (1)$$

where F_i is the non-equilibrium distribution function, F^{eq}_i is the equilibrium distribution function, and $\mathbf{e}_i$ is the microscopic velocity at lattice node $\mathbf{x}$ at time t, respectively, and τ is the relaxation time which is a function of fluid viscosity. In lattice units, fluid viscosity (ν) is function of lattice speed of sound (c_s) and relaxation time (τ) and given as $\nu = c_s^{\,2}(\tau - 0.5)$. The subscript i in Eq.1 represents the lattice directions around the node as shown in Figure 1d. Equilibrium distribution functions for different LB models were derived by He and Luo *(6)*. The function is given in the following form for the two-dimensional model with nine microscopic velocity vectors (D2Q9):

$$\mathrm{F}_i^{eq} = w_i\,\rho\left[1 + 3(\mathbf{e}_i \cdot \mathbf{u}) + \frac{9}{2}(\mathbf{e}_i \cdot \mathbf{u})^2 - \frac{3}{2}(\mathbf{u} \cdot \mathbf{u})\right] \qquad (2)$$

where ρ is the density of the node, and w_i is the weight factor in the i^{th} direction. Weight factors vary for different LB models *(7)*. The weight factors (w_i) for the D2Q9 LB model are: w_9 =16/36 for rest particle, w_i=4/36 ($1 \le i \le 4$) for particles streaming to the face-connected neighbors

and w_i=1/36 $(5 \le i \le 8)$ for particles streaming to the edge-connected neighbors. The weight factors are derived based on the lattice type (DxQy) and the derivations can be found in *(8)*.

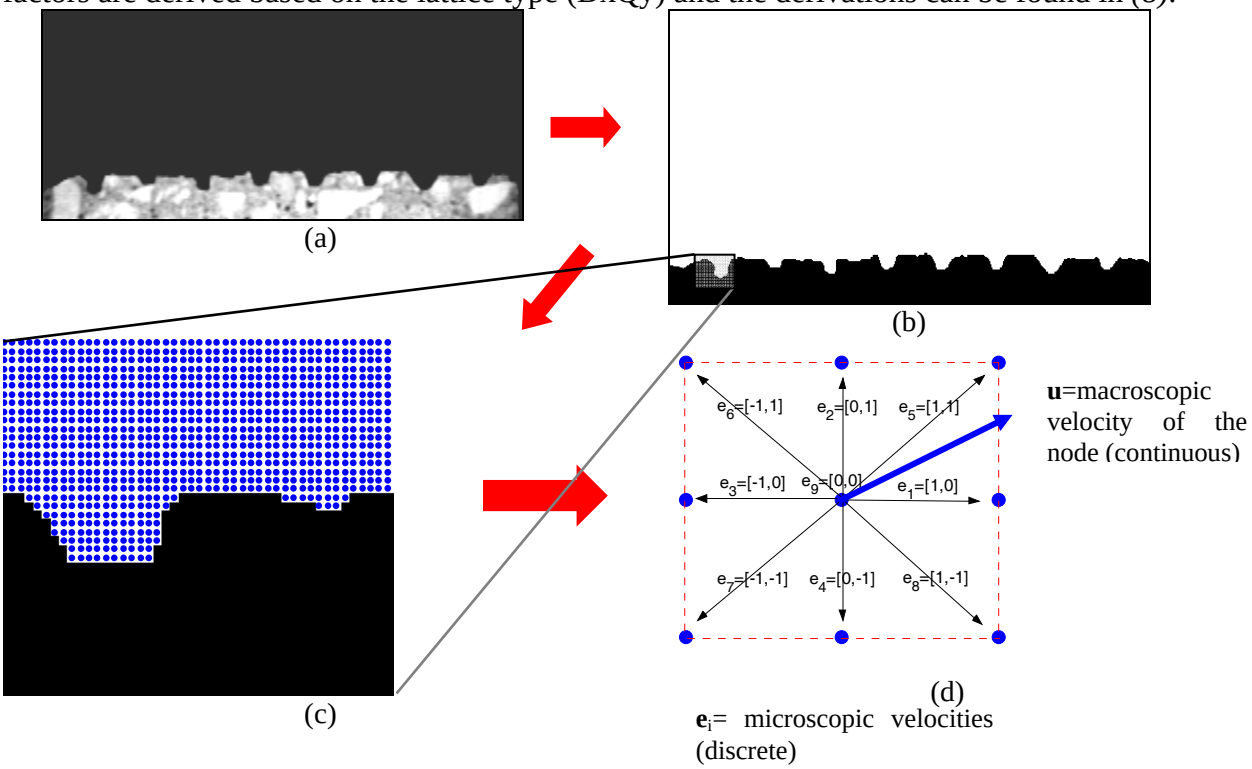

FIGURE 1 (a) Grayscale image of concrete tine surface (b) binary image (black areas represent the solid, and white areas represent the air space) (c) generation of lattice nodes at the center of each white pixel, and (d) D2Q9 lattice microscopic velocity directions defined at each node.

The macroscopic properties, density (ρ), momentum (**U**), and velocity (**u**) of the nodes are calculated using the following relations:

$$\rho = \sum_{i=1}^{Q} \mathrm{F}_i \tag{3}$$

$$\mathbf{U} = \sum_{i=1}^{Q} \left[\mathrm{F}_i \ \mathbf{e}_i\right] \tag{4}$$

$$\mathbf{u} = \frac{\mathbf{U}}{\rho} \tag{5}$$

where Q is the number of microscopic velocities (Figure 1d). Pressure at each lattice node is computed using the equation of state as follows*(4)*:

$$P = {c_s}^2 \rho \tag{6}$$

where P and ρ are pressure and density, respectively, and c_s is the lattice speed of sound that is equal to $1/\sqrt{3}$ for D2Q9 LB model *(4)*.

Detailed description of the steps of a LB algorithm is given elsewhere *(7)*, therefore, it will not be repeated here. A brief description of the steps is as follows:

1. Initially, assign density and velocity to all lattice nodes and calculate initial equilibrium distribution, $F_i^{eq}(\mathbf{x}, t=0)$ using Eq. 2. Then assume initially $F_i(\mathbf{x}, t=0) = F_i^{eq}(\mathbf{x}, t=0)$.
2. Propagate the fluid particles to neighboring nodes by calculating new (non-equilibrium) distribution functions of all nodes using Eq. 1.
3. Calculate new densities and velocities of the nodes using Eq.'s 3 through 5.
4. Impose boundary conditions at the solid/air interface and at domain boundaries.
5. Calculate new equilibrium distribution function of each node using Eq. 2.
6. Repeat steps 2 through 5 until the desired time step.

Kutay et al. *(7)* presented results verifying the accuracy of the D3Q19 LB model for fluid flow problems with well-known analytical and theoretical solutions. An excellent agreement was observed between these solutions and the LB simulations for Stokes flow around a cylinder and flow in circular tubes. The percent error ranged from 0.1% to 2%. It was also shown that the LB model was able to simulate fluid flow accurately, even at very low resolutions (low number of lattice sites). Kutay et al. *(7)* further evaluated the performance of the D3Q19 LB model through laboratory hydraulic conductivity tests conducted on unbound aggregate specimens. X-ray Computed Tomography and mathematical morphology-based techniques were used to analyze the pore structure of the aggregates and these pore structures were input into the LB model. A very good agreement was also observed between the model predictions and the laboratory data.

Modeling of Sound Propagation using Lattice Boltzmann Method

Examples of successful utilization of LB method in sound propagation problems exist in the literature *(14, 15, 16)*, therefore, detailed explanation will not be repeated here. Table 1 shows input parameters required to simulate sound propagation using the LB method. In LB method, the units of density, pressure, distance and time are based on lattice units. In order to obtain the physical units from lattice units (or vice-versa), so-called "resolution parameters" are used. Table 2 presents the resolution parameters as well as the relations used to convert lattice units to physical units. Conversion from physical units to lattice units can easily be performed by simple rearrangement of equations in Table 2. In Table 2, Δx is an input based on the geometry and the selected lattice size. In this study, since the binary images are directly utilized, it corresponds to the resolution of the image in mm/pixel (i.e., the size of one pixel). Another input is the mass resolution (Δm) which was selected to be equal to unity. One of characteristics of the LB method is that the speed of sound in lattice units ($c_{s(L)}$) is constant (for D2Q9 lattice) and equal to $1/\sqrt{3}$. This allows computation of the time resolution (Δt) using the formulation below:

$$\Delta t = \Delta x \frac{c_{s(L)}}{c_{s(w)}} = \Delta x \frac{1}{c_{s(w)}\sqrt{3}} \qquad (7)$$

where $c_{s(L)}$ is the lattice speed of sound, $c_{s(w)}$ is the speed of sound in air (344 m/s), Δt and Δx are the time and spatial resolutions, respectively. Assuming $c_{s(w)}$ =344x10^3 mm/s, time resolution is simply, $\Delta t = \Delta x * 1.68 \times 10^{-6}$. It should be noted that, based on Eq. 7, the time step of the simulations are directly proportional to the spatial resolution. In order to simulate a sound pressure at a frequency of 1000 Hz, assuming a sinusoidal signal and each sinusoid is sampled

about 40 points per cycle (i.e. sampling frequency, f_s = 40), required maximum Δt = 1/1000/40=2.5 x10^{-5} sec (see Figure 2). This corresponds to a spatial resolution of Δx=2.5 x10^{-5} / 1.68 x10^{-6} = 14.9 mm/pixel. By increasing the sampling frequency, the Δt can be reduced, thus the Δx.

TABLE 1. Input air properties for simulation of sound propagation using LB method.

Parameter	Value	Description
$\Delta x = \Delta y$	100	Lattice (spatial) resolution (mm/pixel)
f	1000	Frequency of the applied pressure (Hz)
ρ	1.19E-6	Density of air (g/mm^3)
μ	1.84E-5	Dynamic viscosity of air (Pa-s = g/mm-s)
$\nu = \mu / \rho$	15.46	Kinematic viscosity of air (mm^2/s)
$c_{s(w)}$	344E3	Speed of sound (mm/s) in physical units
P_o	2E-5	Reference pressure (Pa = N/m^2 = g/mm-s^2)
P_{atm}	1E5	Atmospheric pressure (Pa = N/m^2 = g/mm-s^2)
SPL	100	Sound pressure level to be simulated (dB)

TABLE 2. Physical versus lattice units and inter-conversion relationships

Parameter	Physical	Lattice	Resolution parameters used for conversion	Relationship
Distance	x (mm)	(x_L) pixel	Δx	$x = x_L \Delta x$
Time	t (sec)	t_L (time)	Δt	$t = t_L \Delta t$ (t_L = 1, 2, …)
Mass	m (g)	m_L (mass)	Δm = 1	$m = m_L$
Density	ρ (g/mm^3)	ρ_L (mass/pixel^3)	Δm, Δx	$\rho = \rho_L \Delta m / \Delta x^3$
Velocity	v (mm/sec)	v_L(pixel/time)	Δx, Δt	$v = v_L \Delta x / \Delta t$
Pressure	P (Pa= g/mm-s^2)	P_L (mass/pixel-time^2)	Δm, Δx, Δt	$P = P_L \Delta m / (\Delta x \Delta t^2)$
Kinematic Viscosity	ν (mm^2/s)	ν_L(pixel^2/time)	Δx, Δt	$v = v_L \Delta x^2 / \Delta t$

Similar to the calculations above, required resolutions at different frequencies and sampling frequencies for each cycle (i.e., f_s) can be computed. Figure 3 shows the relationship between the frequency of pressure wave, spatial resolution and the sampling frequency of each cycle of the pressure. From this graph, required sampling frequency can be computed for a given selected spatial resolution and the frequency of pressure wave (or vice versa). For example, for a resolution of 10 mm/pixel, and a frequency of 1000 Hz, the required sampling frequency is approximately 10^2. This means that each cycle of pressure wave is simulated in 100 time steps. From this information, the amount of computing time required to perform simulations can be estimated.

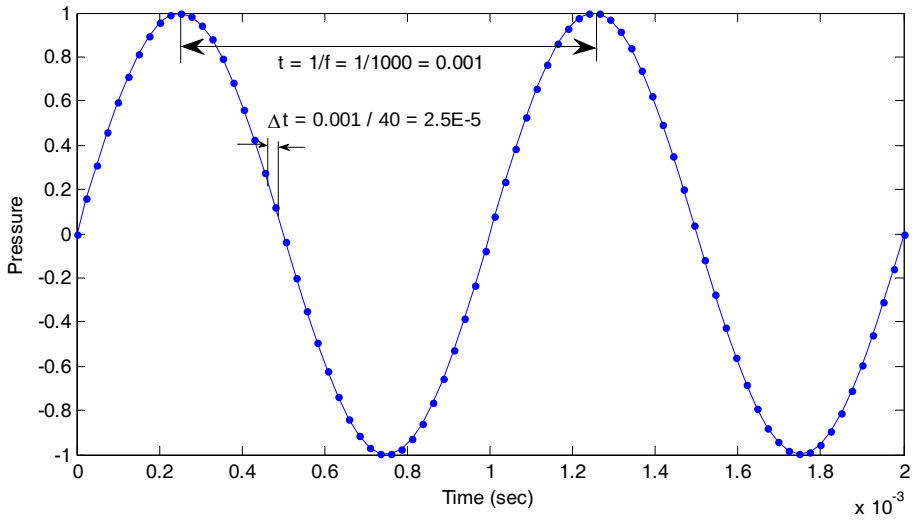

FIGURE 2 Illustration of calculation of required time step for simulation of pressure fluctuations at 1000 Hz.

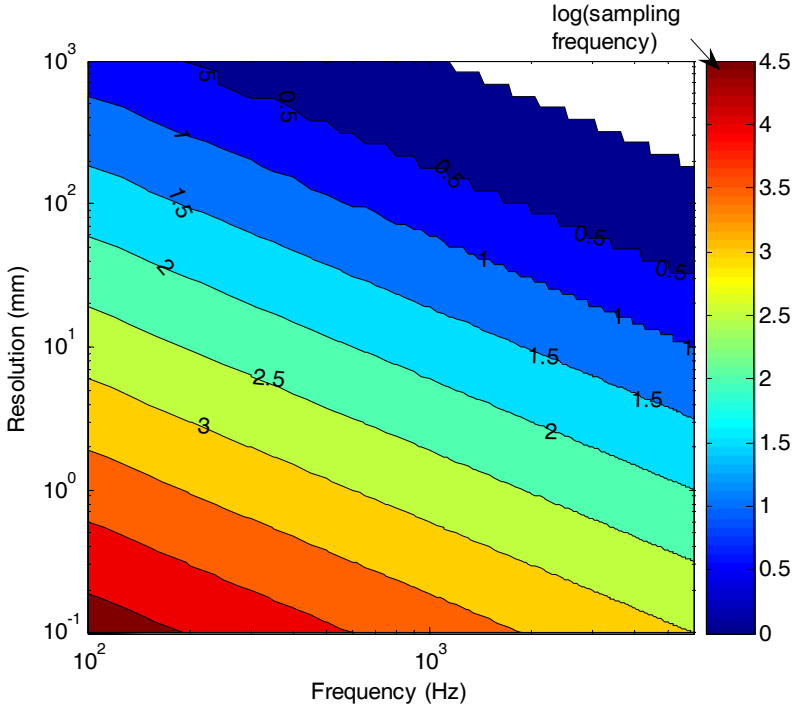

FIGURE 3 Relationship between the pressure frequency, spatial resolution and the sampling frequency of each cycle of the pressure.

Boundary conditions at solid/air interface

In the propagation step of the LB algorithm, all components of the non-equilibrium distribution function are computed at each node except at nodes that are neighbors with solid nodes (Figure 4a). At these nodes, components of the distribution function that are expected to be migrating from the solid node are unknown. In this case, a wall boundary condition is used to calculate the missing components. The most commonly used technique to calculate unknown components of

the distribution function at these nodes is the application of no-slip boundary condition *(9)*. It is also referred to as the bounce-back scheme, in which the distribution function components heading towards the solid nodes scatter directly back to the node. This ensures the conservation of mass, momentum and also ensures zero velocity right at the air/solid interface.

Boundary conditions at domain boundaries

Similar to the solid nodes, certain components of the distribution function of the nodes located at the boundaries of the domain (i.e., left, right, top and bottom nodes) are also unknown as seen in Figure 4b. These components were calculated using the Grad's approximation method *(10)*. Each missing component of the distribution function is computed using the following formula:

$$\mathrm{F}_i^* = w_i \rho \left[1 + \frac{u_\alpha e_{i\alpha}}{c_s^2} + \frac{1}{2c_s^4} (\mathrm{P}_{\alpha\beta} - c_s^2 \delta_{\alpha\beta})(e_{i\alpha} e_{i\beta} - c_s^2 \delta_{\alpha\beta}) \right] \quad (8)$$

$$\mathrm{P}_{\alpha\beta} = \sum_{i=1}^{9} \mathrm{F}_i e_{i\alpha} e_{i\beta} \quad (9)$$

where ρ is the density of the node, and w_i is the weight factor in the i^{th} direction, u is the (macroscopic) velocity of the node, e_i is the microscopic velocity, c_s is the lattice speed of sound and δ is the kronecker delta. Repeating subscripts α and β represent the summation in tensor notation (each representing a component of the vector).

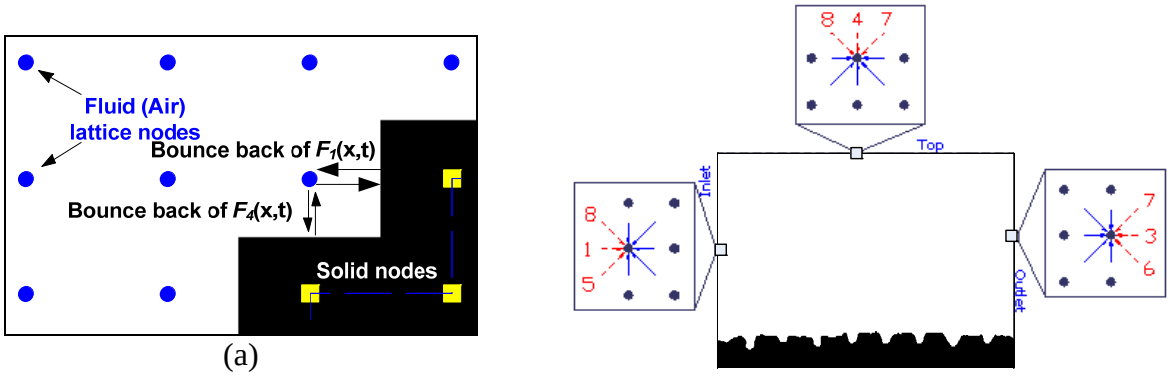

(a) (b)

FIGURE 4 (a) Illustration of solid wall boundary condition and (b) missing components of distribution function at domain boundary conditions.

Validation of LB method using Analytical Solutions

First validation of the algorithms was performed using the propagation of a line source (a point in 2D space) in air. Analytical solution for line source diffraction is given as follows *(11)*:

$$SPL_2 = SPL_1 + 10 \log\left(\frac{d_1}{d_2}\right) \quad (10)$$

where SPL_1 and SPL_2 are the sound pressure levels at distances d_1 and d_2 from the source.

The LB simulations were performed by prescribing sinusoidal pressure fluctuations at a lattice point at the frequency of 100 Hz. A domain of 25 m by 25 m was selected and air

properties given in Table 1 were input. At the center of the domain, pressure values were fluctuated sinusoidally at 100Hz. The amplitude of the pressure level was calculated from the selected SPL using the equation below *(12)* :

$$P = P_o 10^{\frac{SPL}{20}} \quad (11)$$

where P_o is reference pressure (= $2x10^{-5}$ Pa), SPL is the sound pressure level, and P is the amplitude of the pressure to be applied.

Figure 5a shows a snapshot of the air pressure levels propagating during the LB simulation. Simulation was performed for an SPL of 100 dB, corresponding to P = 2 Pa. The d_1 value in Eq. 10 was the distance between the source lattice node and the next, and the SPL_1 value was the sound pressure level at the neighboring node. Figure 5b shows a comparison of LB simulations and the analytical solution given in Eq. 10, where an excellent agreement is visible.

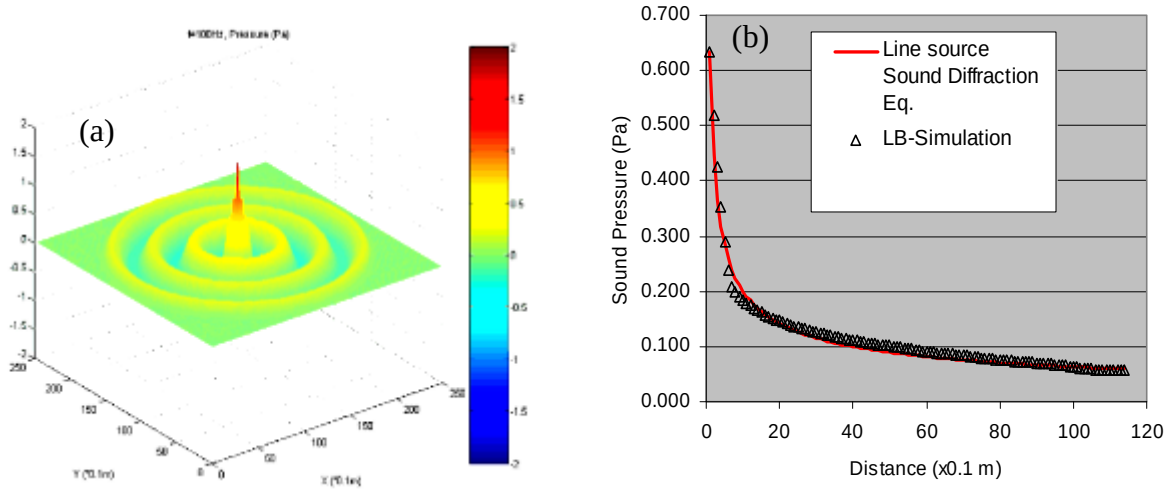

FIGURE 5. (a) Visualization of pressure waves propagating during LB simulations and (b) validation of the LB simulations with the analytical equation.

Validation of LB method through Laboratory Testing

In order to further validate the LB simulations with laboratory data, sound reflection measurements on the surface of a concrete block was conducted. Figure 6a shows the measurement setup where a speaker was placed one end of the concrete block and a sinusoidal sound at a frequency of 1000 Hz and SPL of 70 dB was generated. The microphone configuration measuring the sound level at different distances from the speaker is also shown in Figure 6a. LB simulations were conducted for the same setup and calculated SPL distribution is shown in Figure 6b. Direct comparison of the SPL values calculated at the microphone locations and measured values are shown in Figure 6a. Figure 6a shows that there is a very good agreement between the LB simulations and laboratory data up to a distance of 4 inches, after which the results seem to diverge. LB model currently implemented in this study is two dimensional, which provides cylindrical propagation of sound waves. Whereas, laboratory sound propagation is spherical. Therefore, this difference is expected.

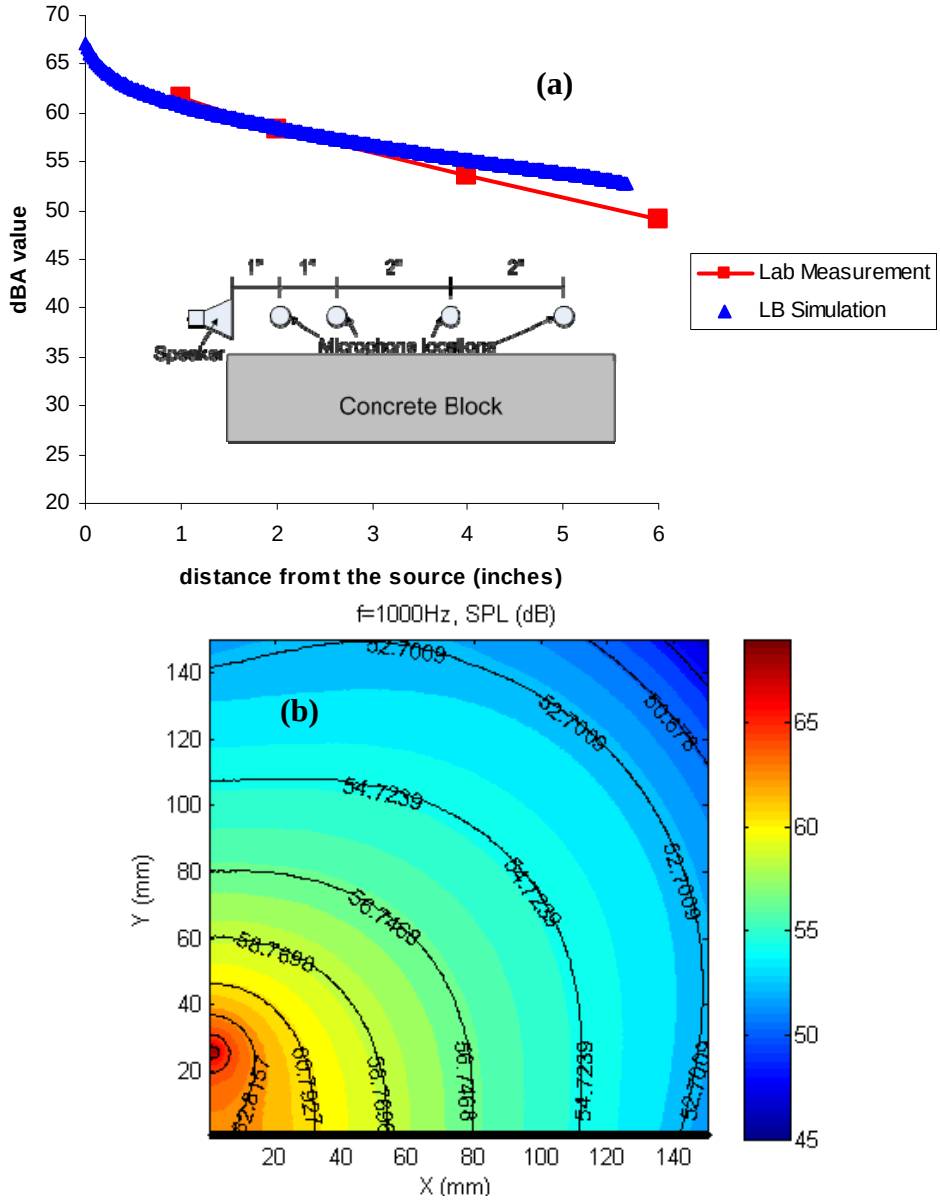

FIGURE 6 (a) Microphone configuration for the laboratory sound reflection tests and the comparison between the laboratory measured and LB simulated values, and (b) a snapshot of the SPL distribution from the LB simulation.

LB SIMULATIONS OF SOUND DIFFRACTION ABOVE DIFFERENT PAVEMENT SURFACES

Effect of Tine Spacing and Depth

In order to investigate the effect of the tine spacing and depth of concrete pavements on the propagation of sound, LB simulations were conducted on different geometries with different tine spacing and depth. The source was placed 1 inch above the surface and a sound pressure level of 90 dB at 1000Hz was emitted. Then the SPLs were recorded through virtual microphones placed at 1 inch from the surface at different distances from the source. Figure 7 shows the simulation results where the difference on the reflection of sound waves seems to be minimal for different

tine spacing and depths. Propagation of sound in air (with no surface) is also shown in Figure 7 for comparison purposes. It is noted that, in LB simulations, the pavement surface was assumed to reflect all the sound waves (i.e., no absorption). In addition, the environmental factors such as the wind and temperature variations are ignored.

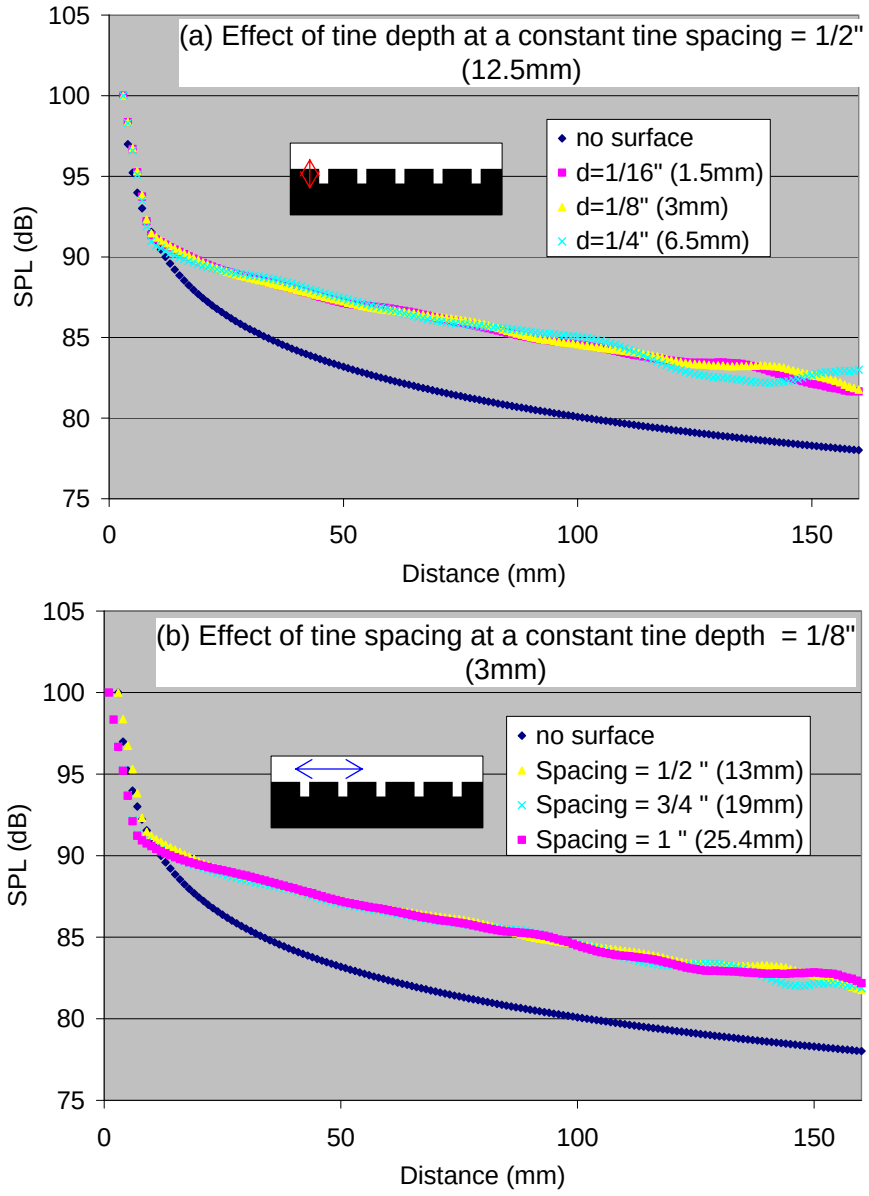

FIGURE 7 LB simulation results showing the effect of (a) tine depth and (b) spacing on the propagation of sound.

Effect of Different Pavement Surfaces

In order to study the effect of different surface types, LB sound propagation simulations were conducted above three different types of surfaces: (1) a tined surface, (2) porous surface and (3) a surface with horn-shaped grooves. Figure 8 shows the results of the simulations. The red solid line in the graph represents the sound propagation when there is no surface, i.e., free propagation of sound in air. As seen from Figure 8 that the porous surface absorbs the sound waves much

more than the other surface types. This is consistent with the field experience and common knowledge. The horn-shaped surface and the tined surface seemed to be similar at distances less than 30 mm. After 30 mm, the SPL values for horn-shaped surface fluctuate above the SPL values of tined surface. This is possibly due to the amplification of sound waves by the horn-shaped surface.

It should be noted that many other types of surfaces can be input to the model in the form of a binary (black and white) image, similar to the images shown in Figure 8. Currently, this model is in 2D but can be (and will be) extended to 3D easily. Real pore geometries of different pavement surfaces can be generated by scanning field cores using X-ray Computed Tomography (CT) equipment. Then 3D images can be converted to binary images and directly be input the LB model as illustrated in Figure 1.

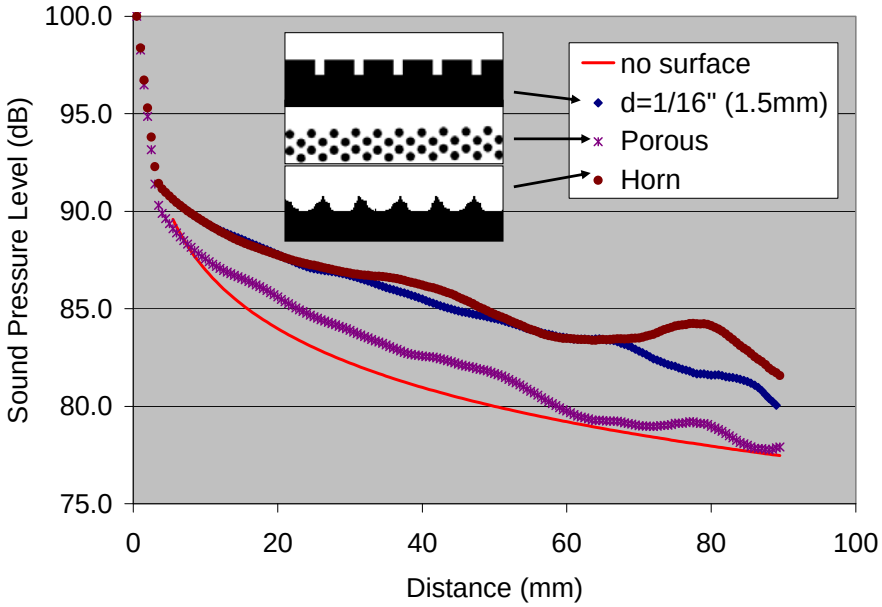

FIGURE 8 LB simulations of sound propagation and absorption on various surface types.

EXAMPLE APPLICATIONS OF LB METHOD FOR MODELING SOUND PROPAGATION AND GENERATION

There are numerous application areas for LB method in modeling sound propagation. Examples include the environmental impact studies of roadways and other noise sources, development of noise maps, and barrier design…etc. Figure 9 shows example simulations of propagation of roadway noise into the nearby regions. In Figure 9a, it was assumed that solid regions are rigid and reflect the pressure waves 100%. Whereas, in Figure 9b, an absorption coefficient was assigned to the solid regions (i.e., pavement, wall and trees). The absorption coefficient in simulation shown in Figure 9b was implemented through a momentum sink applied to Eq. 4 at the nodes corresponding to these regions. When Figure 9a and Figure 9b are compared, the effect of absorption of sound on the SPL distribution in the environment can easily been quantified.

Since the LB method produces an explicit solution of air flow and resulting pressure distribution, it is relatively easy to simulate the generation of sound waves as well. Even though it hasn't been extensively studied in this research, preliminary simulations showed great promise on simulation of generation of sound. Figure 10 shows pressure contours generated due to the rotating tire on a pavement computed by the LB simulations. In these simulations the tire is assumed to be rigid and an angular velocity as well as a linear velocity at the center was assigned

such that it simulates the rotation and translation of tire. The specific boundary conditions used in simulating rotating tire were the same ones for the suspension flow presented in Kutay and Aydilek *(13)*. Transient nature of the pressure contours due the movement of rotating tire creating sound waves can be observed in Figure 10. It should be noted that LB method can simulate some of the noise generating mechanisms such as the horn effect, air pumping, pipe resonance…etc. However, it doesn't currently include some other important mechanisms such as stick-snap (adhesion) and the vibration of the tire threads *(1)*. These other mechanisms can be implemented into the LB model by incorporating a model that can provide the deformation behavior of tire at these lattice nodes. This could possibly be done by coupling the LB method with a finite element method.

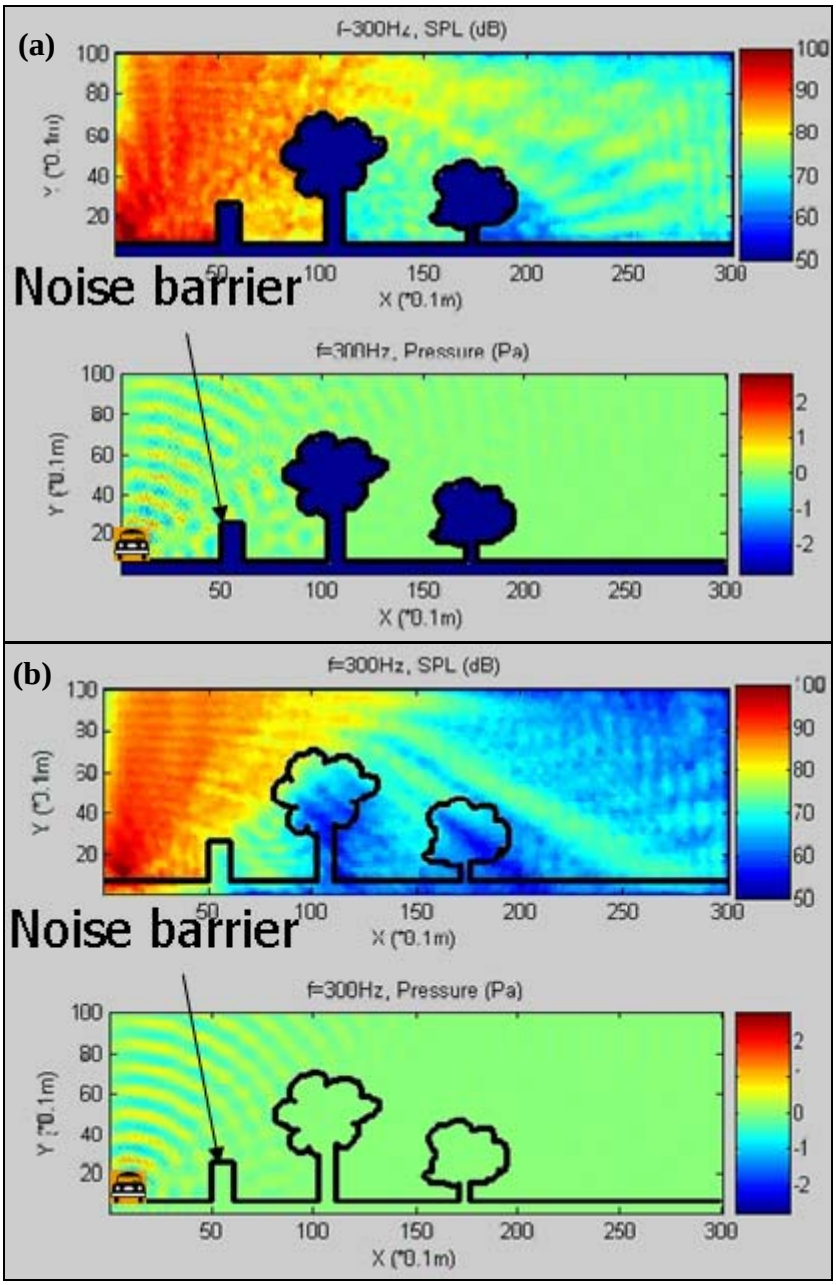

FIGURE 9 LB Simulations of traffic noise: (a) full reflection from the solid regions and (b) partial absorption at the pavement, wall and trees.

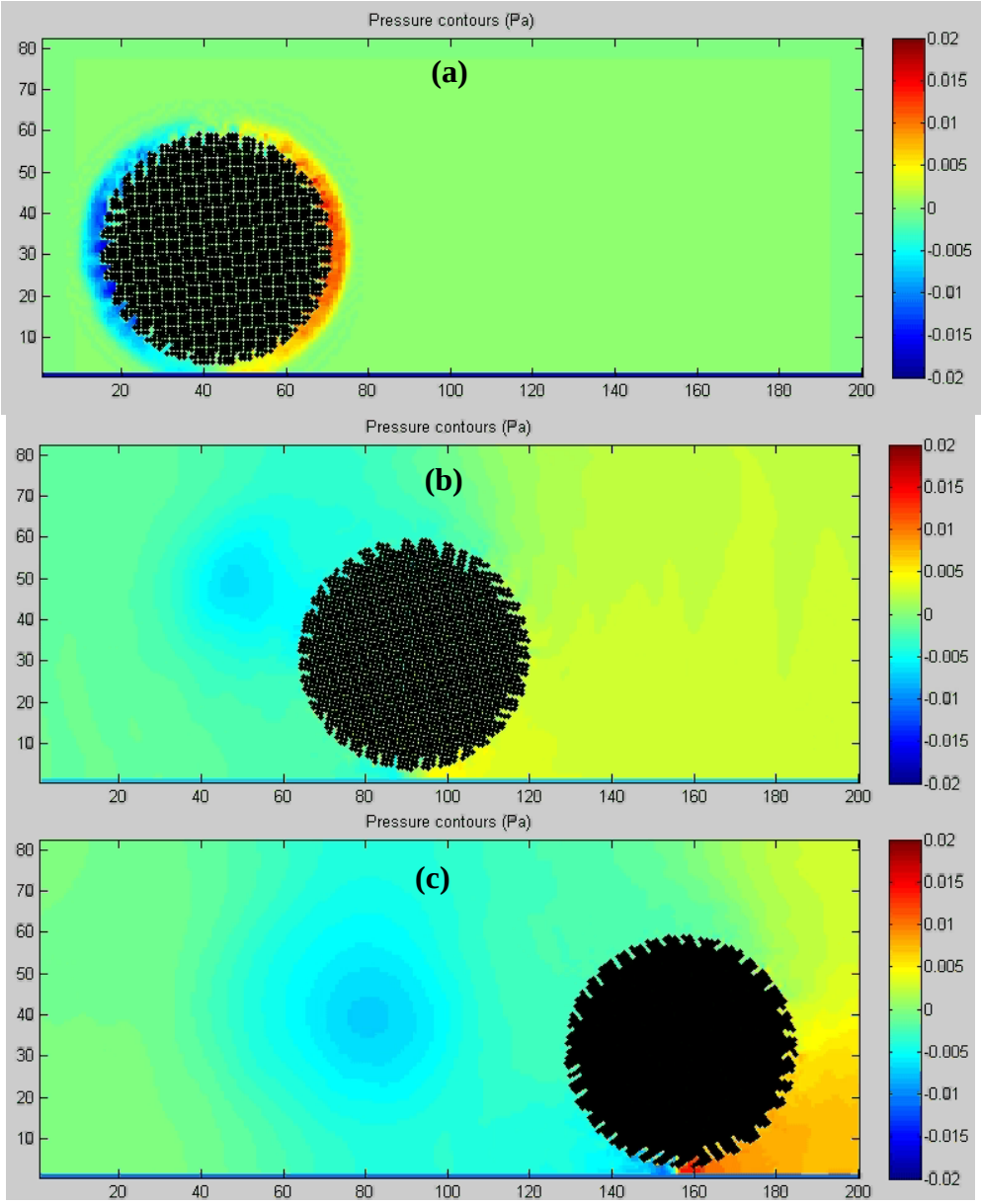

FIGURE 10 Pressure contours generated due to the rotating tire on a pavement computed by the LB simulations.

CONCLUSIONS

This paper presented a new approach, the Lattice Boltzmann (LB) method, for modeling sound propagation and generation from the roadways. The theory of LB method and its application to sound wave problems have been presented in detail. The accuracy of the LB model was verified against well-known analytical solution of propagation of a line source. The performance of the LB model was further evaluated by comparing the results of the simulations to laboratory measurements of sound diffraction above a concrete block. A very good agreement was observed between the model predictions and the laboratory measurements. The LB algorithm was then utilized to study the effects of different pavement surface types on the propagation of sound. It

was observed that tine spacing and depth did not have a significant effect on the propagation of sound above tined concrete pavements. On the other hand, the simulations of sound above a porous pavement showed significant absorption of sound as compared to the other surface types, which is consistent with the field experience and common knowledge. Lastly, several example applications of LB method for sound propagation as well as sound generation problems were presented.

REFERENCES

(1) Sandberg, U. and Ejsmont, J. A. (2002), Tyre/road Noise Reference Book, Informex, Ejsmont & Sandberg Handelsbolag, Kisa, Sweden.

(2) Ferragut, T. Rasmussen, R.O., Wiegand, P., Mun, E. and Cackler, E. T. (2007) ISU-FHWA-ACPA Concrete Pavement Surface Characteristics Program Part 2: Preliminary Field Data Collection. FHWA report for DTFH61-01-X-00042 (Project 15, Part 2).

(3) Succi S. (2001). "The Lattice Boltzmann Equation: for Fluid Dynamics and Beyond", Series Numerical Mathematics and Scientific Computation, Oxford University Press, Oxford-New York.

(4) Maier, R., Kroll, D., Kutsovsky, Y., Davis, H. T., and Bernard, R. (1997). "Simulation of Flow through Bead Packs Using the Lattice Boltzmann Method", AHPCRC Preprint 97-034, Univ. of Minnesota.

(5) McNamara, G. and Zanetti, G. (1988). "Use of the Boltzmann Equation to Simulate Lattice-Gas Automata", Phys. Rev. Lett., Vol. 61, pp. 2332-2335.

(6) He, X.and Luo, L. (1997) "Theory of Lattice Boltzmann Method: From the Boltzmann Equation to the Lattice Boltzmann", *Phys. Rev. E,* Vol. 56, pp. 6811-6817.

(7) Kutay, M.E. Aydilek, A.H. and Masad, E. (2006). "Laboratory validation of lattice Boltzmann method for modeling pore-scale flow in granular materials", Computers and Geotechnics.Vol. 33, pp 381-395.

(8) Wolf-Gladrov, D. A. (2000). "Lattice-Gas Cellular Automata and Lattice Boltzmann Models: An Introduction" Springer, Berlin.

(9) Maier RS, Bernard RS, Grunau DW. (1996) "Boundary conditions for the lattice Boltzmann method". Physics of Fluids Vol. 8, No. 7, pp. 1788–801.

(10) Chikatamarla, S.S., Ansumali, S. and Karlin, I.V. (2006) "Grad's approximation for missing data in lattice Boltzmann simulations", Europhysics Letters, Vol. 74, No. 2, pp. 215-221.

(11) Lee, C. S.Y. and Fleming, G. G. (1996). Measurement of Highway-Related Noise. Report No. FHWA-PD-96-046 and DOT-VNTSC-FHWA-96-5. Cambridge, MA: John A. Volpe National Transportation Systems Center, Acoustics Facility, May 1996.

(12) Fleming, G.G., Knauer, H.S., Lee, C.S. and Perdersen, S. (2000). FHWA Highway Noise Barrier Design Handbook.

(13) Kutay, M.E. and Aydilek, A. H. (2008) "Numerical Modeling of Suspensions using the Lattice Boltzmann Method", *ASCE GeoCongress 2008*, March 9-12, 2008, New Orleans, LA.

(14) Buick, J.M., Greated, C.A. and Campbell, D. M. (1998) “Lattice BGK simulation of sound waves”, *Europhysics Letters,* Vol. 43, No. 3, pp. 235-240.

(15) Buick, J. M. , C. L. Buckley, C. A. Greated, and J. Gilbert, “Lattice Boltzmann BGK simulation of nonlinearsound waves: the development of a shock front,” *Journal of Physics A: Mathematical and General*, vol. 33,pp. 3917–3928, 2000.

(16) Haydock, D and J. Yeomans, “Lattice Boltzmann simulations of acoustic streaming,” *Journal of Physics A: Mathematics and General*, vol. 34, pp. 5201–5213, 2001.